

18. Datar, S. A., Jacobs, H. W., de La Cruz, A. F., Lehner, C. F. & Edgar, B. A. The *Drosophila* cyclin D–cdk4 complex promotes cellular growth. *EMBO J.* **19**, 4543–4554 (2000).
19. Meyer, C. A. *et al.* *Drosophila* cdk4 is required for normal growth and is dispensable for cell cycle progression. *EMBO J.* **19**, 4533–4542 (2000).
20. Johnson, R. L., Grenier, J. K. & Scott, M. P. *patched* overexpression alters wing disc size and pattern: transcriptional and post-transcriptional effects on *hedgehog* targets. *Development* **121**, 4161–4170 (1995).
21. Kenney, A. M. & Rowitch, D. H. Sonic hedgehog promotes G(1) cyclin expression and sustained cell cycle progression in mammalian neuronal precursors. *Mol. Cell. Biol.* **20**, 9055–90567 (2000).
22. Milenkovic, L., Goodrich, L. V., Higgins, K. M. & Scott, M. P. Mouse *patched1* controls body size determination and limb patterning. *Development* **126**, 4431–4440 (1999).
23. Fantl, V., Stamp, G., Andrews, A., Rosewell, I. & Dickson, C. Mice lacking cyclin D1 are small and show defects in eye and mammary gland development. *Genes Dev.* **9**, 2364–2372 (1995).
24. Donnellan, R. & Chetty, R. Cyclin E in human cancers. *FASEB J.* **13**, 773–780 (1999).
25. Wang, T. C. *et al.* Mammary hyperplasia and carcinoma in MMTV–cyclin D1 transgenic mice. *Nature* **369**, 669–671 (1994).
26. Xu, T. & Rubin, G. M. Analysis of genetic mosaics in developing and adult *Drosophila* tissues. *Development* **117**, 1223–1237 (1993).
27. Struhl, G. & Basler, K. Organizing activity of wingless protein in *Drosophila*. *Cell* **72**, 527–540 (1993).
28. Patel, N. In *In situ Hybridization to Whole Mount Drosophila Embryos* (ed. Krieg, P. A.) 357–370 (Wiley-Liss, New York, 1996).
29. Bosco, G., Du, W. & Orr-Weaver, T. L. DNA replication control through interaction of E2F-RB and the origin recognition complex. *Nature Cell Biol.* **3**, 289–295 (2001).
30. Johnston, L. A. & Edgar, B. A. Wingless and Notch regulate cell-cycle arrest in the developing *Drosophila* wing. *Nature* **394**, 82–84 (1998).

Supplementary Information accompanies the paper on Nature's website (<http://www.nature.com>).

Acknowledgements

We thank J. Jiang, B. Edgar, C. Lehner, R. Holmgren, H. Richardson, T. Kornberg and the Bloomington Stock Center for providing fly stocks and antibodies used in this study. We gratefully acknowledge C. Heitzig and M. Giorgianni, who performed preliminary experiments that contributed to this work. C. Gudanowski provided technical assistance. We thank E. Williamson and the University of Chicago scanning electron microscope facility, as well as J. Auger and the University of Chicago Flow Cytometry Facility, for their technical advice. We are grateful for discussions with members of the Du lab, the Patel lab, and the Center for Molecular Oncology. Comments from C. Ferguson, A. Mahowald, N. Dyson and J. Duman aided us in the preparation of this manuscript. We thank B. Edgar for communicating results to us before publication. Grants from the American Cancer Society and the National Institutes of Health to W.D. supported this work.

Competing interests statement

The authors declare that they have no competing financial interests.

Correspondence and requests for materials should be addressed to W.D. (e-mail: wdu@ben-may.bsd.uchicago.edu).

TREX is a conserved complex coupling transcription with messenger RNA export

Katja Sträßer^{*†‡}, Seiji Masuda^{†‡}, Paul Mason^{†§}, Jens Pfannstiel^{*}, Marisa Oppizzi^{*}, Susana Rodriguez-Navarro^{*}, Ana G. Rondón^{||}, Andres Aguilera^{||}, Kevin Struhl[§], Robin Reed[‡], & Ed Hurt^{*}

^{*} BZH, University of Heidelberg, Im Neuenheimer Feld 328, D-69120 Heidelberg, Germany

[‡] Department of Cell Biology; and [§] Department of Biological Chemistry and Molecular Pharmacology, Harvard Medical School, Boston, Massachusetts 02115, USA

^{||} Department of Genetics, University of Sevilla, E-41012 Sevilla, Spain

[†] These authors contributed equally to this work

The essential yeast proteins Yra1 and Sub2 are messenger RNA export factors that have conserved counterparts in metazoans, designated Aly and UAP56, respectively^{1–7}. These factors couple the machineries that function in splicing and export of mRNA^{1–7}. Here we show that both Yra1 and Sub2 are stoichiometrically associated with the heterotetrameric THO complex⁸, which functions in transcription in yeast^{8–11}. We also show that Sub2

and Yra1 interact genetically with all four components of the THO complex (Tho2, Hpr1, Mft1 and Thp2). Moreover, these components operate in the export of bulk poly(A)⁺ RNA as well as of mRNA derived from intronless genes. Both Aly and UAP56 associate with human counterparts of the THO complex. Together, these data define a conserved complex, designated the TREX ('transcription/export') complex. The TREX complex is specifically recruited to activated genes during transcription and travels the entire length of the gene with RNA polymerase II. Our data indicate that the TREX complex has a conserved role in coupling transcription to mRNA export.

Proteins that interact with Sub2 in yeast were detected by a single-step protein A (ProtA) affinity purification method, which resulted in the identification of Yra1 and several uncharacterized proteins (Fig. 1a, lane 1)⁷. To determine whether the latter proteins specifically associate with Sub2, we employed the more stringent tandem affinity purification (TAP) method for detecting protein interactions, which involves two sequential affinity purification steps¹². Using TAP-tagged Sub2, we detected a significant enrichment of six major proteins that were observed in the original ProtA affinity purification (Fig. 1a, compare lanes 1 and 3)⁷. Consistent with previous studies⁷, one of these proteins is Yra1. The others were a previously unknown open reading frame (ORF) (*YNL253w*)—hereafter designated Tex1 (for Trex component)—Tho2, Hpr1, Mft1 and Thp2 (Fig. 1a, lane 3). The latter four proteins are all components of the THO complex, which functions in transcription elongation^{8–10,13,14}. Mutations in THO-complex components markedly decrease RNA levels of a *GAL1–lacZ* reporter without affecting promoter function, a phenotype also observed in strains lacking the well-characterized elongation factor TFIIS (ref. 15). In addition, THO-complex mutants are sensitive to the drug 6-azauracil⁹ (K.S., unpublished data), as observed for TFIIS and other transcription elongation factors¹⁵. Finally, THO-complex components interact genetically with Srb2, Srb5, Hrs1, Gal11 and Sin4, which are subunits of the mediator complex required for transcription^{10,13,14,16}.

The observation that a complex that functions in transcription elongation interacts with mRNA export factors raises the possibility that the export factors are recruited to mRNAs by a transcription-coupled mechanism. So we further characterized these interactions. To investigate the specificity of the association between Sub2 and the THO complex, we TAP-tagged Tho2, Hpr1, Mft1 and Thp2, and identified the proteins that are bound in yeast cells. As expected, the other three components of the THO complex co-purified with each of the tagged proteins (Fig. 1a, lanes 4–7). Sub2, Yra1 and Tex1 were also identified in each pulldown assay (Fig. 1a, lanes 4–7). These proteins are approximately stoichiometric with the four components of the THO complex. Moreover, purification of Sub2 from yeast strains lacking single THO-complex components (*hpr1Δ*, *mft1Δ* and *thp2Δ*) causes a complete loss of interaction of the remaining subunits of the THO complex, including Tex1 (see Supplementary Information Fig. 1). We conclude that the THO complex interacts with Sub2 and that Tex1 does not independently interact with Sub2. Finally, the interaction of Sub2, Yra1 and Tex1 with the THO complex is insensitive to RNase (data not shown). We conclude that the THO complex interacts specifically with Sub2 and Yra1 *in vivo*. We have designated this complex TREX because it contains factors involved in both mRNA export and transcription.

To further characterize the TREX complex, we analysed the proteins present after purification from yeast cells by column chromatography, including a stringent 1 M salt elution⁸. All four components of the THO complex were detected on a silver-stained gel (Fig. 1b). In addition, western analysis of this preparation detected Sub2. In contrast, Yra1 was not detected (Fig. 1b). We conclude that Sub2 is more tightly associated with the TREX complex than is Yra1. Thus, Sub2 may mediate the interaction between the THO complex and Yra1.

The mRNA export machinery is conserved between yeast and

humans¹⁷. Thus, we next asked whether the TREX complex exists in humans. Previous pulldown assays from HeLa cell nuclear lysates using glutathione *S*-transferase (GST)–UAP56 identified Aly and additional proteins⁶. Further characterization of these proteins on a low-percentage SDS–polyacrylamide gel revealed two highly specific bands, which migrated at relative molecular mass (*M_r*) values of about 180,000 (180K) and about 90K (Fig. 1c, lane 4). On a higher-percentage gel, these two bands, a specific band at about 45K, and Aly were detected (Fig. 1d, lane 4). The 180K band

corresponds to a protein whose partial human chromosomal DNA sequence was recently reported as a potential Tho2 homologue¹¹. We constructed a full-length complementary DNA encoding this protein and aligned it with other Tho2 homologues, revealing significant levels of conservation throughout the protein (see Supplementary Information Fig. 2). The 90K band contains peptides that correspond to a new human protein whose full-length cDNA sequence is present in the GenBank database (<http://www.ncbi.nlm.nih.gov/Genbank>). On the basis of the alignment of this protein with other ORFs in the database, the 90K protein is an apparent human homologue of Hpr1 (see Supplementary Information Fig. 3). Finally, the 45K band corresponds to a protein whose full-length cDNA is also present in the database. The closest homologue to this human cDNA encodes the yeast *Tex1* protein (see Supplementary Information Fig. 4). Apparent metazoan homologues of Mft1 and Thp2 are not present in the database, and we have not detected them in the UAP56 pulldown assay. We conclude that UAP56 associates with human homologues of Tho2, Hpr1 and *Tex1*. Consistent with our yeast data, the interaction of UAP56, Aly, human (h) Tho2, hHpr1 and h*Tex1* was not abolished by RNase treatment of HeLa nuclear lysates (Fig. 1e). We conclude that the TREX complex, containing components of both the mRNA export and transcription machineries, is conserved from yeast to humans. The conservation of this complex suggests that it is critical in mediating interactions between transcription and mRNA export.

Genetic studies in yeast indicate that the biochemical interactions that define the TREX complex are functionally significant. Specifically, we identified all four components of the THO complex in a

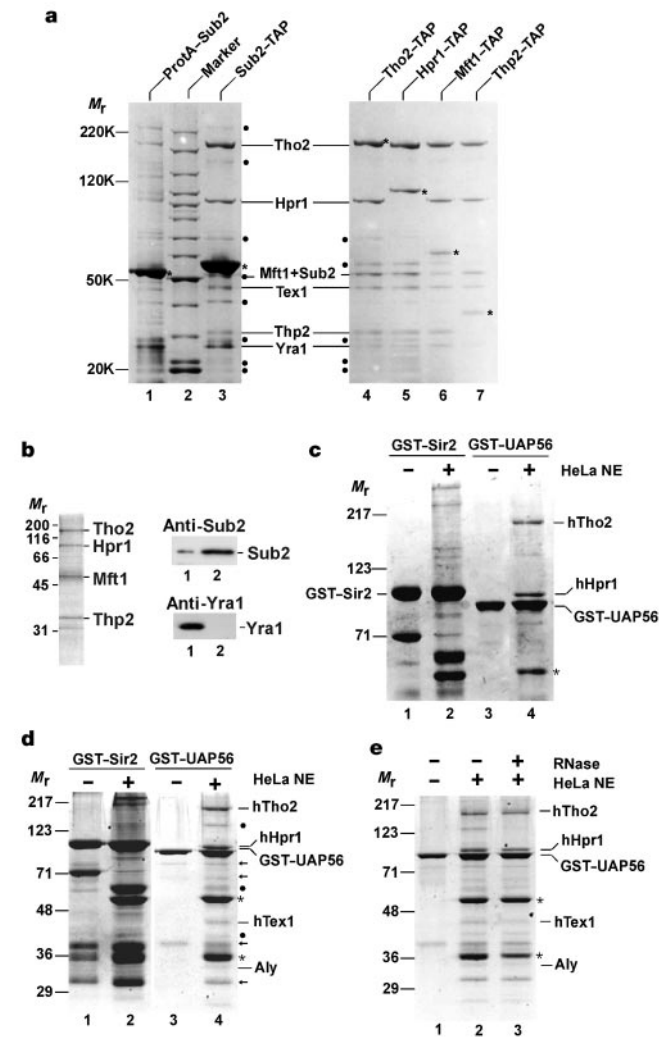


Figure 1 Identification of the conserved TREX complex. **a**, Proteins associated with ProtA–Sub2 (ref. 7) (lane 1) or the indicated TAP-tagged proteins (lanes 3–7) isolated from yeast. Major co-purifying proteins are indicated. Lower-abundance proteins are indicated by filled circles: (from top to bottom) Mlp1 (lane 3), Sac3 (lane 3), Hsp70 (lanes 3–7), Hrb1 (lanes 4–7), Gbp2 (lane 3; co-migrates with Mft1), breakdown product of Sub2 (lane 3) and three ribosomal L-proteins. Asterisks, tagged proteins. **b**, Column chromatography-purified TREX complex analysed by SDS–polyacrylamide gel electrophoresis (PAGE) and silver stained (left) or by western blot using Sub2 and Yra1 antibodies (right). **c, d**, control GST–Sir2 (lanes 1 and 2) or GST–UAP56 (lanes 3 and 4) were incubated with buffer (–) or with HeLa nuclear extract (NE) (+). Proteins bound to GST–UAP56 (lane 4) were analysed by 6.5% (**c**) or 10% (**d**) SDS–PAGE. Human (h) Tho2 (AF441770), hHpr1 (Q9UPZ5) and h*Tex1* (MGC5469) are indicated (see Supplementary Information Figs 2–4). ORF I39463 co-migrates with hHpr1. The lower-abundance proteins are indicated by filled circles: (from top to bottom) Q9BXP4, β -tubulin and MGC2655. Asterisks, abundant lysate proteins. Arrows, breakdown products of GST–UAP56. **e**, GST–UAP56 incubated with buffer (–) or HeLa NE (+), in the absence (–) or presence (+) of RNase.

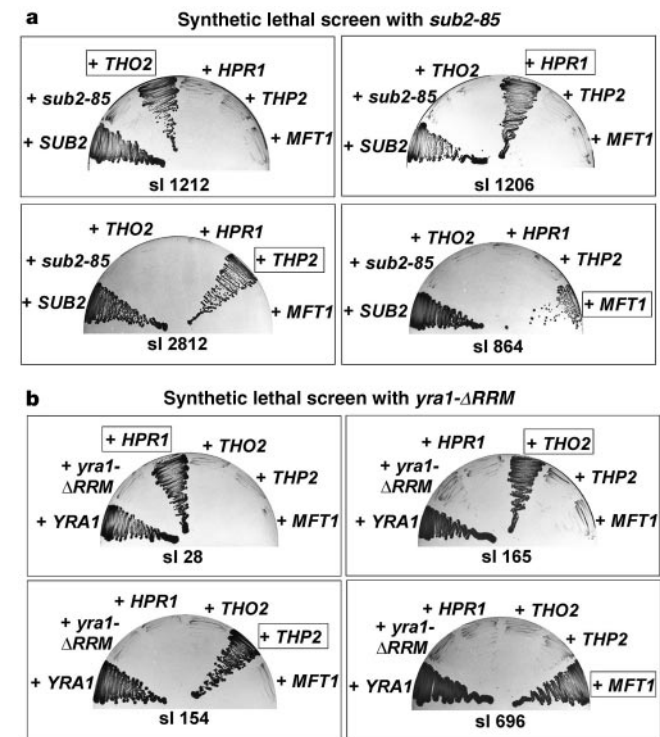


Figure 2 *SUB2* and *YRA1* interact genetically with the genes encoding the four components of the THO complex. **a**, Synthetic lethal screen with the *sub2-85* allele performed at 23 °C. Synthetic lethal (sl) strains 1202, 1206, 2812 and 864 were transformed with plasmids encoding *SUB2*, *sub2-85*, *THO2*, *HPR1*, *MFT1* and *THP2*. **b**, Synthetic lethal screen with the *yra1-ΔRRM* allele performed at 30 °C. Synthetic lethal strains 28, 154, 165 and 696 were transformed with plasmids encoding *YRA1*, *yra1-ΔRRM*, *THO2*, *HPR1*, *MFT1* and *THP2*. Rescue of the synthetic lethal phenotype was assessed by growth after 5 days on plates containing 5-fluoroorotic acid (5-FOA). No growth indicates synthetic lethality.

synthetic lethal screen using a thermosensitive mutant of Sub2, *sub2-85*, which is defective in mRNA export (Fig. 2a)⁷. In this screen, we isolated 28 synthetic lethal mutants. Five of these were complemented by *HPR1*, four by *THO2*, two by *MFT1*, and two by *THP2* (Fig. 2a). This finding is supported by studies showing that *SUB2* is a high copy suppressor of *hpr1* mutants¹⁴.

We next asked whether THO complex components interact genetically with *YRA1*. We previously carried out a synthetic lethal screen with a *yra1* allele, *yra1-ΔRRM*, which lacks the RNA recognition motif (RRM)⁷. This screen led to the identification of Sub2 (ref. 7). Three of the uncharacterized synthetic lethal mutants from this screen were complemented by *THP2* and two by *HPR1* (Fig. 2b). The other two components of the THO complex, *THO2* and *MFT1*, were identified in another synthetic lethal screen with the *yra1-ΔRRM* mutant (Fig. 2b). We conclude that Sub2 and Yra1 interact not only physically but also genetically with the THO complex.

Consistent with our observations linking the THO complex to mRNA export factors, an *hpr1* mutant was previously shown to have an mRNA export defect¹⁸. This defect was detectable because the *hpr1* mutant, like the other THO complex mutants, impairs but does not abolish transcription^{8–10}. To determine whether the other components of the THO complex also have a role in mRNA export, we tested thermosensitive mutants for an mRNA export defect. Some accumulation of poly(A)⁺ RNA was detected in the nucleus at permissive temperature (30 °C), and after a 2-h shift to restrictive temperature (37 °C), a stronger accumulation was observed with the *tho2*, *hpr1*, *mft1* and *thp2* mutants (Fig. 3a). We conclude that all four components of the THO complex function in mRNA export.

Although Sub2/UAP56 was identified as an essential splicing

factor in yeast and metazoans^{19–22}, this protein is required for export of both spliced mRNAs and mRNAs derived from intronless genes^{4–7}. Thus, we next asked whether the THO complex mutants affect export of the heat shock *SSA1* mRNA, which is derived from an intronless gene. To induce transcription of *SSA1* mRNA, wild-type yeast or the THO complex mutants were shifted to the restrictive temperature. *SSA1* mRNA accumulates in the nucleus of each mutant, but not in wild-type cells (Fig. 3b). We conclude that the THO complex is required for efficient export of mRNAs derived from intronless genes.

Studies of the THO components of the TREX complex, together with our observation that mRNA export factors are associated with this complex, raise the possibility that the TREX complex operates in coupling transcription elongation to mRNA export. To address this possibility, we used an *in vivo* assay to determine whether the TREX complex associates with an actively transcribed gene and moves along the gene with RNA polymerase II. We performed a chromatin immunoprecipitation assay in strains containing a long (~8 kilobases) yeast gene (ORF *YLR454*) under the control of the regulatable *GAL1* promoter (Fig. 4a). The strains expressed tagged Hpr1–Myc or Tho2–Myc, from genes integrated into the chromosome. *YLR454* expression was induced by shifting the cells from raffinose- to galactose-containing medium. After induction, the *GAL1* promoter was turned off by addition of glucose to the medium. As shown in Fig. 4b, RNA polymerase II, Hpr1 and Tho2 are not associated with the reporter gene in raffinose (Ref lanes). However, all three proteins associate with the entire region of the transcribing gene in galactose (Gal lanes) as shown with the 5′-, middle-, and 3′-specific polymerase chain reaction (PCR) primers. On addition of glucose, RNA polymerase II, Hpr1 and Tho2 are cleared from the 5′ to the 3′ end of the gene in a time-dependent manner (4-min and 15-min Glu lanes). We conclude that the TREX complex is specifically recruited to the transcribing gene and travels with the polymerase during transcriptional elongation.

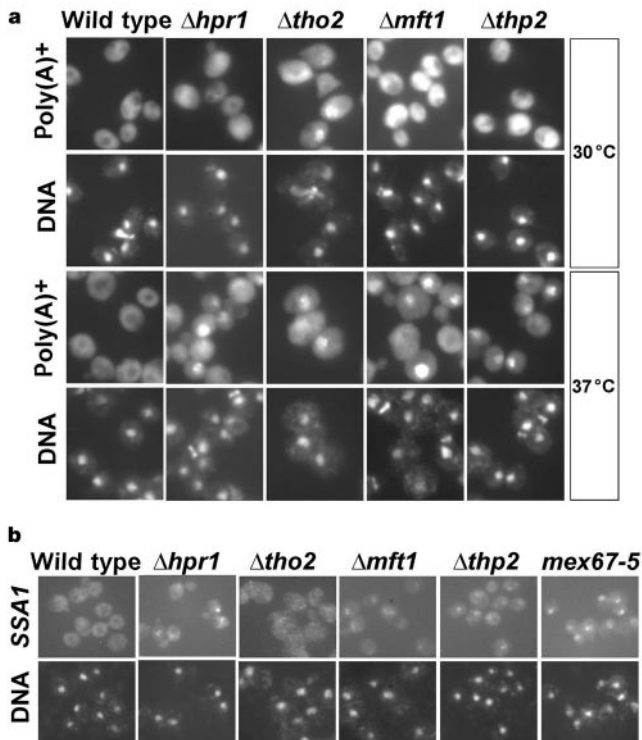


Figure 3 Deletion of *THO2*, *HPR1*, *MFT1* or *THP2* results in an mRNA export defect. **a**, Wild-type yeast (strain W303), $\Delta tho2$, $\Delta hpr1$, $\Delta mft1$ and $\Delta thp2$ strains were grown at 30 °C or shifted for 2 h to 37 °C. Localization of poly(A)⁺ RNA was assessed by *in situ* hybridization. DNA was stained with 4,6-diamidino-2-phenylindole (DAPI). **b**, Accumulation of intronless heat shock *SSA1* mRNA in the nucleus in wild-type, $\Delta tho2$, $\Delta hpr1$, $\Delta mft1$ and $\Delta thp2$ strains, which were grown at 30 °C and shifted for 30 min to 42 °C, as assessed by *in situ* hybridization. The DNA was stained with DAPI.

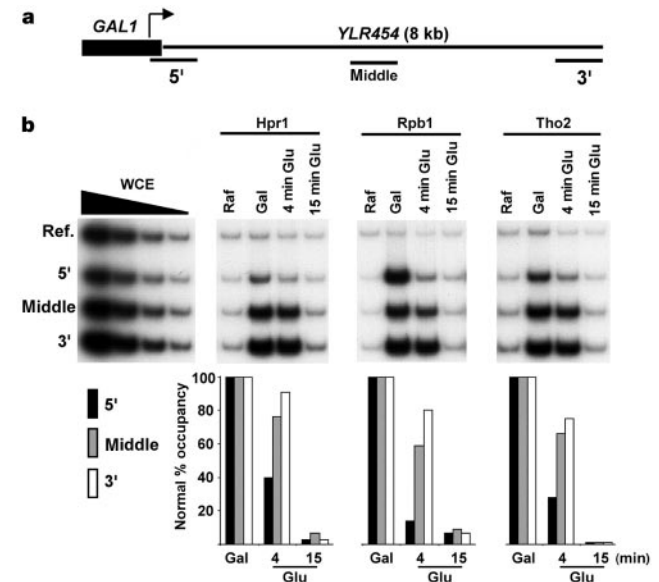


Figure 4 TREX components are recruited to active genes. **a**, Schematic diagram of *GAL1::YLR454* reporter showing primers used for chromatin immunoprecipitation. **b**, *GAL1::YLR454* cells containing Hpr1–Myc or Tho2–Myc were treated with formaldehyde after growth in raffinose followed by glucose addition for 15 min, or after galactose induction followed by 0, 4 or 15 min of glucose incubation. Chromatin was immunoprecipitated with Myc or polymerase II antibodies and PCR was performed using the indicated primers. Immunoprecipitations were quantified and are displayed as the remaining percentage of galactose-induced protein occupancy at each region of the gene at 0, 4 or 15 min after addition of glucose. Ref., reference (see Methods).

The TREX complex physically links proteins that function either in mRNA export or transcription. Two components of the TREX complex, Yra1 and Sub2, are required for mRNA export^{4–7}. A third component, Tex1, is new. Finally, four of the components—Tho2, Hpr1, Mft1 and Thp2—are constituents of the THO complex, which functions in transcription elongation^{8–10,13,14}. The human TREX complex contains Aly, UAP56, hTex1, hTho2 and hHpr1. The remarkable conservation of the TREX complex from yeast to humans reveals the importance of the association of mRNA export and transcription components in the same complex. This conclusion is underscored by our observation that all four components of the THO complex interact genetically with both *YRA1* and *SUB2*. Recent studies in yeast have also identified a link between transcription and mRNA export²³. This work revealed that Npl3 interacts with RNA polymerase II and that both Npl3 and Yra1 are recruited to mRNA during transcription²³. However, the mechanism for this recruitment is not known. Our studies suggest that the conserved TREX complex may be a principal mediator in coupling transcription to mRNA export. In support of this conclusion, our data show that the TREX complex is recruited to actively transcribed genes, where this complex travels with the elongating polymerase along the entire length of the gene. Components of the TREX complex function in export of mRNAs derived from naturally intronless genes as well as bulk poly(A)⁺ mRNA. Thus, it is possible that the TREX complex has a conserved role in loading the mRNA export machinery on to both intron-containing and intron-lacking pre-mRNAs. □

Methods

Yeast analysis

The *Δyra1 ade2 ade3* and the *sub2* shuffle strains were described⁷ as W303, *Δtho2*, *Δhpr1*, *Δmft1* and *Δthp2*^{8,10}. The *Δsub2 ade2 ade3* strain for the synthetic lethal screen with *sub2-85* was created by mating the *SUB2* shuffle strain to strain JB²⁴ and tetrad analysis. The TAP tag was integrated into the genome carboxy-terminal of the *SUB2*, *THO2*, *HPRI1*, *MFT1* and *THP2* genes by homologous recombination as described¹². Plasmids pUN100-*YRA1* (ref. 1), pRS315-*THO2* (ref. 10), pHT4467-*YRA1*, pRS314-*yra1-ΔRRM* and pRS314-*sub2-85* (ref. 7) were described previously. pHT4467Δ-*SUB2* was constructed by subcloning the *SUB2* ORF containing the *SacI*-*XhoI* fragment of pUN100-*SUB2* into the *SacI* and *XbaI* sites of pHT4467Δ (ref. 24). The synthetic lethal screen and oligo(dT) *in situ* hybridization¹ and *in situ* hybridization with the Cy3-labelled oligonucleotides recognizing the *SSA1* transcript was performed as described⁷.

Protein purification and mass spectrometry

TAP-tagged proteins were purified essentially as described¹². Proteins associated with the purified TAP-tagged proteins were identified by mass spectrometry, which was performed as described²⁴. GST-UAP56 pulldown assays from HeLa nuclear extracts were performed as described⁶. The His-tagged Tho2-purified THO complex was obtained from the strain SchY73 following a described procedure⁶ but using 1 M potassium acetate for elution from the BIO Rex 70 column. Western analysis was performed using polyclonal anti-Sub2 and anti-Yra1 antibodies. Sequence comparison was performed using ClustalW 1.8 (BCM Search Launcher; <http://dot.imgen.bcm.tmc.edu/multi-align/multi-align.html>) and BOXSHADE 3.21 (http://www.ch.embnet.org/software/BOX_form.html) for printing and shading of multiple alignment files.

Cloning of human Tho2

A partial human cDNA (CAA19741) encoding hTho2 is present in the GenBank database. To obtain a full-length Tho2 cDNA clone, ORF CAA19741 was used to identify XM-047325, which contains the start codon of hTho2. PCR was then used to isolate the full-length human Tho2 cDNA from a HeLa cDNA library using primers 5'-ATGTTTGTTCAGACACAGTCTAAAGGAA and 5'-GATGGAAAGTCTCATATTCTGCTGTGTC.

Chromatin immunoprecipitation

GAL1::YLR454 cells containing Hpr1-13-Myc or Tho2-13-Myc were grown in synthetic medium containing 2% raffinose. Culture portions (20 ml) were treated for 20 min with 1% formaldehyde, followed by addition of 360 mM glycine. Crosslinked cells were washed twice with cold TBS (20 mM Tris buffer at pH 7.5, 150 mM NaCl). Cell pellets were resuspended in lysis buffer (50 mM HEPES at pH 7.5, 150 mM NaCl, 1 mM EDTA, 0.1% SDS, 0.1% deoxycholate, 1 mM phenylmethylsulphonyl fluoride) and lysed with a mini bead-beater, followed by sonication sufficient to produce DNA fragments of an average size of 500 base pairs (bp). We used 60% of each soluble extract for immunoprecipitation

with polyclonal anti-Myc antibodies (Upstate Biotechnology), and 15% of each extract was used for immunoprecipitation with anti-Rpb1 antibodies (8WG16, Covance). Immunoprecipitation and PCR were performed as described²⁵. Immunoprecipitated samples and twofold dilutions of whole-cell extract (WCE) were analysed by PCR using primers spanning the *SSA4* promoter ('reference' in Fig. 4b; 300 bp), the *YLR454* translation start codon ('5'' in Fig. 4; 235 bp), the approximate mid-point of the *YLR454* ORF ('middle'; 200 bp), and the *YLR454* translation stop codon ('3''; 150 bp). The data were quantified by phosphorimager and are displayed as the remaining percentage of galactose-induced protein occupancy at each region of the gene at 0, 4 or 15 min after addition of glucose.

Received 12 March; accepted 16 April 2002.

Published online 28 April 2002, DOI 10.1038/nature746.

1. Straßer, K. & Hurt, E. C. Yra1p, a conserved nuclear RNA binding protein, interacts directly with Mex67p and is required for mRNA export. *EMBO J.* **19**, 410–420 (2000).
2. Stutz, F. *et al.* REF, an evolutionarily conserved family of hnRNP-like proteins, interacts with TAP/Mex67p and participates in mRNA nuclear export. *RNA* **6**, 638–650 (2000).
3. Zhou, Z. L. *et al.* The protein Aly links pre-messenger-RNA splicing to nuclear export in metazoans. *Nature* **407**, 401–405 (2000).
4. Gatfield, D. *et al.* The DEXH/D box protein HEL/UAP56 is essential for mRNA nuclear export in *Drosophila*. *Curr. Biol.* **11**, 1716–1721 (2001).
5. Jensen, T. H., Boulay, J., Rosbash, M. & Libri, D. The DECD box putative ATPase Sub2p is an early mRNA export factor. *Curr. Biol.* **11**, 1711–1715 (2001).
6. Luo, M.-J. *et al.* Pre-mRNA splicing and mRNA export linked by direct interactions between UAP56 and Aly. *Nature* **413**, 644–647 (2001).
7. Straßer, K. & Hurt, E. C. Splicing factor Sub2p is required for nuclear export through its interaction with Yra1p. *Nature* **413**, 648–652 (2001).
8. Chávez, S. *et al.* A protein complex containing Tho2, Hpr1, Mft1 and a novel protein, Thp2, connects transcription elongation with mitotic recombination in *Saccharomyces cerevisiae*. *EMBO J.* **19**, 5824–5834 (2000).
9. Chavez, S. & Aguilera, A. The yeast *HPRI1* gene has a functional role in transcriptional elongation that uncovers a novel source of genome instability. *Genes Dev.* **11**, 3459–3470 (1997).
10. Piruat, J. I. & Aguilera, A. A novel yeast gene, THO2, is involved in RNA pol II transcription and provides new evidence for transcriptional elongation-associated recombination. *EMBO J.* **17**, 4859–4872 (1998).
11. West, R. W., Kruger, B., Thomas, S., Ma, J. & Milgrom, E. RLR1 (THO2), required for expressing lacZ fusions in yeast, is conserved from yeast to humans and is a suppressor of SIN4. *Gene* **243**, 195–205 (2000).
12. Rigaut, G. *et al.* A generic protein purification method for protein complex characterization and proteome exploration. *Nature Biotechnol.* **17**, 1030–1032 (1999).
13. Chang, M. *et al.* A complex containing RNA polymerase II, Paflp, Cdc73p, Hpr1p, and Ccr4p plays a role in protein kinase C signalling. *Mol. Cell. Biol.* **19**, 1056–1067 (1999).
14. Fan, H. Y., Merker, R. J. & Klein, H. L. High-copy-number expression of Sub2p, a member of the RNA helicase superfamily, suppresses hpr1-mediated genomic instability. *Mol. Cell. Biol.* **21**, 5459–5470 (2001).
15. Kulish, D. & Struhl, K. TFIIIS enhances transcriptional elongation through an artificial arrest site *in vivo*. *Mol. Cell. Biol.* **21**, 4162–4168 (2001).
16. Piruat, J. I., Chavez, S. & Aguilera, A. The yeast *HRS1* gene is involved in positive and negative regulation of transcription and shows genetic characteristics similar to *SIN4* and *GAL11*. *Genetics* **147**, 1585–1594 (1997).
17. Reed, R. & Hurt, E. C. A conserved mRNA export machinery coupled to pre-mRNA splicing. *Cell* **108**, 523–531 (2002).
18. Schneider, R. *et al.* The *Saccharomyces cerevisiae* hyperrecombination mutant *hpr1Δ* is synthetically lethal with two conditional alleles of the acetyl coenzyme A carboxylase gene and causes a defect in nuclear export of polyadenylated RNA. *Mol. Cell. Biol.* **19**, 3415–3422 (1999).
19. Fleckner, J., Zhang, M., Valcarcel, J. & Green, M. R. U2AF65 recruits a novel human DEAD box protein required for the U2 snRNP-branchpoint interaction. *Genes Dev.* **11**, 1864–1872 (1997).
20. Kistler, A. L. & Guthrie, C. Deletion of MUD2, the yeast homolog of U2AF65, can bypass the requirement for Sub2, an essential spliceosomal ATPase. *Genes Dev.* **15**, 42–49 (2001).
21. Libri, D., Graziani, N., Saguez, C. & Boulay, J. Multiple roles for the yeast *SUB2/yUAP56* gene in splicing. *Genes Dev.* **15**, 36–41 (2001).
22. Zhang, M. & Green, M. R. Identification and characterization of yUAP/Sub2p, a yeast homolog of the essential human pre-mRNA splicing factor hUAP56. *Genes Dev.* **15**, 30–35 (2001).
23. Lei, E. P., Krebber, H. & Silver, P. A. Messenger RNAs are recruited for nuclear export during transcription. *Genes Dev.* **15**, 1771–1782 (2001).
24. Baßler, J. *et al.* Identification of a 60S pre-ribosomal particle that is closely linked to nuclear export. *Mol. Cell* **8**, 517–529 (2001).
25. Kuras, L. & Struhl, K. Binding of TBP to promoters *in vivo* is stimulated by activators and requires Pol II holoenzyme. *Nature* **399**, 609–613 (1999).

Supplementary Information accompanies the paper on Nature's website (<http://www.nature.com>).

Acknowledgements

We are grateful to J. Lechner for assistance in the mass spectrometry, J. Bassler for initial help in this project and G. B. Winkler and J. Q. Svejstrup for their help in the isolation of the His-tagged THO complex. E.H. was supported by grants from the Deutsche Forschungsgemeinschaft (SFB, Gottfried Wilhelm Leibniz-Program) and Fonds der Chemischen Industrie; A.A. by grants from the Spanish Ministry of Science and Technology and the Human Frontier Science Program; R.R. and K.S. by National Institutes of Health (NIH) grants. S.M. is supported by the fellowship programme for Japanese scholars and researchers and P.M. is supported by an NIH postdoctoral fellowship.

Competing interests statement

The authors declare that they have no competing financial interests.

Correspondence and requests for materials should be addressed to R.R. (e-mail: rreed@hms.harvard.edu), K.S. (e-mail: Kevin@hms.harvard.edu) or E.H. (e-mail: cg5@ix.urz.uni-heidelberg.de).

The dynamics of actin-based motility depend on surface parameters

Anne Bernheim-Groswasser*, Sebastian Wiesner†, Roy M. Golsteyn*‡, Marie-France Carlier† & Cécile Sykes*

* Laboratoire Physico-chimie 'Curie', UMR 168 CNRS/Institut Curie, 11, rue Pierre et Marie Curie, 75231 Paris cedex 05, France
 † Dynamique du Cytosquelette, Laboratoire d'Enzymologie et Biochimie Structurales, UPR A 9063 CNRS, 91198 Gif-sur-Yvette, France

In cells, actin polymerization at the plasma membrane is induced by the recruitment of proteins such as the Arp2/3 complex, and the zyxin/VASP complex^{1–3}. The physical mechanism of force generation by actin polymerization has been described theoretically using various approaches^{4–6}, but lacks support from experimental data. By the use of reconstituted motility medium⁷, we find that the Wiskott–Aldrich syndrome protein^{8,9} (WASP) sub-domain, known as VCA, is sufficient to induce actin polymerization and movement when grafted on microspheres. Changes in the surface density of VCA protein or in the microsphere diameter markedly affect the velocity regime, shifting from a continuous to a jerky movement resembling that of the mutated 'hopping' *Listeria*¹⁰. These results highlight how simple physical parameters such as surface geometry and protein density directly affect spatially controlled actin polymerization, and play a fundamental role in actin-dependent movement.

Investigations of the pathogens *Listeria monocytogenes* and *Shigella flexneri* were important in identifying many proteins that control cellular actin polymerization and cell motility. These bacteria move within a cell by inducing actin polymerization at their surface¹¹ by way of the activation of the Arp2/3 complex^{12,13}. Immunolocalization studies of the Arp2/3 complex in the lamellipodium¹⁴ show that Arp2/3 multiplies the filaments by branching them in a dendritic array¹⁵, as confirmed by biochemical experiments^{16,17}. More recently, surfaces coated with proteins that induce actin polymerization were used to identify new molecular partners for actin polymerization and assembly¹⁸, or to visualize microscopically the actin network formed at the surface¹⁹.

Here we consider how the surface concentration of Arp2/3 complex activator, or the curvature of the surface on which filament branching and growth occur, can affect and control actin-based movement. We have used beads of various diameters (1–10 μm) grafted with the VCA fragment (VCA indicates verprolin-homology, cofilin-homology, and acidic regions), which constitutively activates Arp2/3 complex. We placed the beads in a medium containing a minimal number of purified proteins that support the movement of *L. monocytogenes* or *S. flexneri*⁷. After a certain time that depends on their size, the beads generated behind them a comet (tail) made of actin filaments and started moving. We identified three main characteristic regimes of motion: continuous (smooth), intermittent or erratic, and periodic or saltatory movement. We believe that this is the first evidence that transition from

continuous to saltatory movement can be achieved simply by a change in a physical parameter—that is, the surface density or the bead diameter.

The VCA-coated beads¹⁸ (1–10 μm in diameter) all had the same saturating surface density C_s of VCA, as confirmed by SDS–polyacrylamide gel electrophoresis (SDS–PAGE) (data not shown). We placed the beads in the mixture of purified proteins⁷, and found that the bead size had a significant effect on the movement type and the comet structure (Fig. 1). Small beads (1–2 μm diameter) moved steadily at a constant velocity (Fig. 1a), as reported in other experimental systems²⁰. Unexpectedly, larger beads displayed a jerky motion. The irregularities in the movement are illustrated by the irregular density (grey level) of the comet (Fig. 1b and c). Furthermore, beads larger than 4.5 μm diameter moved in a periodic hopping manner (Fig. 1c), very similar to the movement of mutated 'hopping' *Listeria*¹⁰. For intermediate-sized beads (3 μm in diameter), a transient or even chaotic movement was observed: the beads hopped randomly, fluctuating from smooth to jerky movement (Fig. 1b). All beads of the same nominal diameter developed comets and showed the same type of motion when sampling the microscope field of view (typically up to 50 beads), showing the robustness of the system.

In these experiments, the surface density of VCA proteins on beads of different diameter was $C_s = (6 \pm 1) \times 10^{-2}$ molecules nm^{-2} . This value corresponds to a maximal surface concentration of VCA. The capacity of immobilized VCA to activate Arp2/3 was evaluated and compared with the activity of VCA in the soluble form using the fluorescence of pyrenyl-actin to monitor the polymerization process. The assay was carried out with identical amounts of immobilized or soluble VCA in parallel. This proved that the specific activity of VCA was the same in both cases, and that the surface concentration of active VCA was independent of the size of the bead.

Mean velocity values, V_{mean} , of beads moving in the solution of purified proteins are given in Table 1. This mean velocity is linearly dependent on the inverse bead diameter. Beads of 1 μm diameter placed in the mixture of purified proteins or in HeLa cell extracts (prepared as previously described²¹) moved with the same average velocity. But in purified protein solution, 100% of the beads started moving by breaking the surrounding symmetrical actin gel ('symmetry breaking') within a few minutes, whereas in the case of cell extracts, symmetry breaking occurred only after 20 minutes and for less than 10% of the beads. Moreover, the velocity fluctuations in the movement of a single bead were 70% in purified proteins as compared to 15% in cell extracts. This can be related to the lower viscosity of the purified protein mixture, as shown in a recent

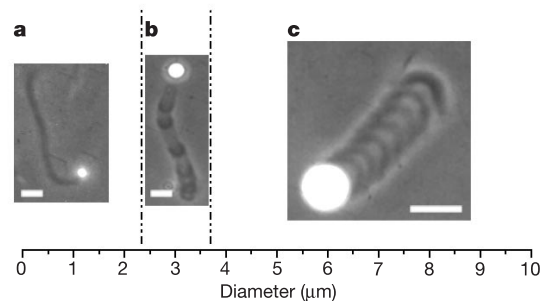


Figure 1 The three main regimes of motion of the beads as a function of bead diameter. In all cases, the beads have a saturated surface concentration of VCA. The dashed vertical lines mark the approximate boundaries between these regimes. **a**, Small beads (<math>< 2.5 \mu\text{m}</math> diameter) with a comet of constant gel density (grey level) exhibit continuous motion. **b**, Medium-size beads of 3 μm diameter move in an intermittent manner, as manifested by the irregular gel density of the comet. **c**, Large beads (>math>\ge 4.5 \mu\text{m}</math> diameter) progress in periodic fashion, as reflected by the alternating comet grey level. Scale bars: **a** and **b**, 5 μm; **c**, 10 μm.

‡ Present address: Division de Cancérologie Expérimentale, Institut de Recherches Servier, 125, chemin de Ronde, 78290 Croissy-sur-Seine, France.